

Quantum control of fast vibrational wavepackets: simulations to establish key experimental observables and constraints

Contact c.calvert@qub.ac.uk

**C. R. Calvert, R. B. King,
J. D. Alexander, O. Kelly,
L. Graham, J. F. McCann,
J. B. Greenwood and I. D. Williams**

*School of Mathematics and Physics,
Queen's University Belfast, University
Road, Belfast, BT7 1NN, UK*

W. A. Bryan and G. R. A. J Nemeth
*Department of Physics, Swansea
University, Singleton Park, Swansea,
SA2 8PP, UK*

W. R. Newell
*Department of Physics and Astronomy,
University College, London, Gower
Street, London, WC1E 6BT, UK*

T. Birkeland
*Department of Mathematics, University
of Bergen, N-5007 Bergen, Norway*

Introduction

Developments in ultrashort-pulse laser technology continue to provide powerful new tools and techniques for steering molecular dynamics. The ability to conduct such studies with femtosecond pulses has provided many advances in ultrafast quantum manipulation of molecules, such as impulsive control of bond orientation^[1], control of electron localisation during dissociation^[2], control of dissociation energetics^[3] and spectral pulse-shaping as an adaptive tool for controlling molecular fragmentation^[4].

For many experiments in this research area, ultrashort pulse interactions not only serve to manipulate molecular behaviour in a coherent manner, but are also crucial for time-resolved imaging of consequent wavepacket dynamics. In one recent example the most fundamental molecular vibrations in nature have been experimentally mapped in time, as reported in previous CLF annual reports^[5,6] and elsewhere^[7,8,9,10,11]. In these studies, few-cycle (≤ 12 fs) intense ($\sim 10^{14}$ W cm⁻²) pulses of infra-red radiation were used to create and image a coherent superposition of vibrational states in the prototypical molecular ion (H_2^+)^[7] and its isotopologues HD^+ ^[8] and D_2^+ ^[5,6,9,10,11,12].

With the most highly resolved experimental observations achieved in D_2^+ ^[9,10] (largest reduced mass), attention has been turned to the prospect of exerting coherent strong-field control over the broad distribution of vibrational states in the wavepacket. Theoretical studies to this end have been documented in recent journal articles^[13-18] and CLF reports^[19,20], where the possible outcomes of applying an ultrashort control pulse have been considered. It has been proposed that, through careful timing of a control pulse, the D_2^+ wavepacket (occupying as many as 10 vibrational states or more) may be coherently quenched towards a single chosen state^[13,15] or into a two-state superposition^[14]. Another fascinating outcome has been identified where the wavepacket may be driven into a coherent superposition of either exclusively even or exclusively odd states, displayed in a so-called 'quantum chessboard'^[16]. A quasi-classical technique^[18] has also been developed for simulating non-destructive wavepacket control and shows

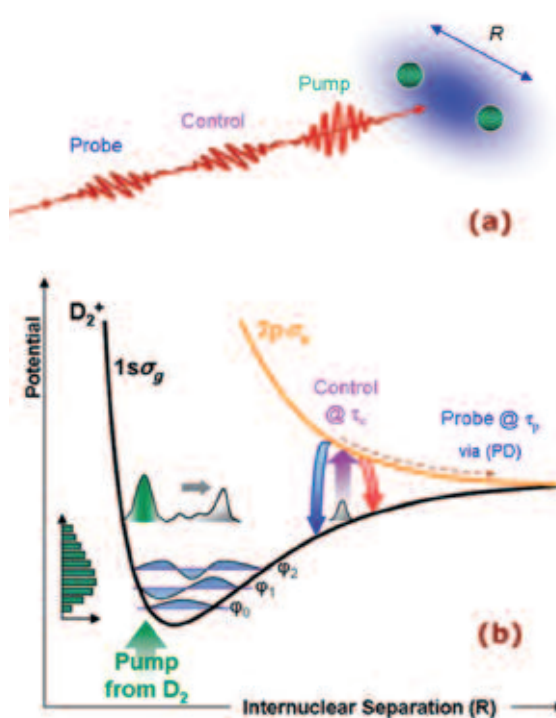


Figure 1. Creation and control of D_2^+ vibrations. The pump pulse launches a wavepacket in a coherent superposition of states on the $1s\sigma_g$ potential. This is allowed to evolve across the potential for some time τ_c prior to application of a control pulse. The modified wavepacket can then be characterised via a probe pulse interaction as a function of delay time τ_p , providing dissociation via the $2p\sigma_u$ surface (dashed line).

excellent agreement with computationally-intensive quantum simulations.

Although experimental control of the D_2^+ wavepacket has been demonstrated through selective dissociation^[3,21] and electron localisation^[2], success has been limited regarding state-selective redistribution of wavepacket population^[19]. With this in mind, we have set out to specifically establish conditions whereby experimental control of vibrational dynamics in the

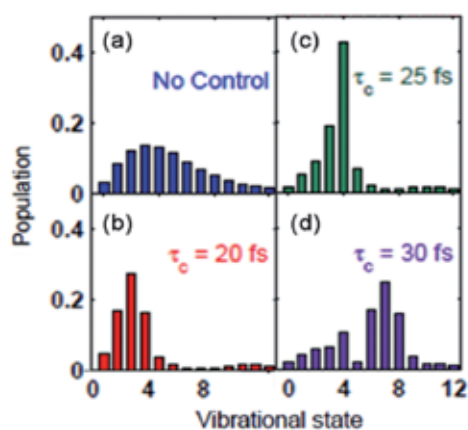


Figure 2. Vibrational distributions of D_2^+ wavepacket. (a) If only the pump pulse is applied (with no subsequent control pulse) the molecule evolves in the FC distribution. As an example of state-selective manipulation, the effect of a 12 fs control pulse of $1 \times 10^{14} \text{ W cm}^{-2}$ peak intensity has been modelled for delay times of (b) 20 fs (c) 25 fs and (d) 30 fs, resulting in notably different final distributions. (Note that no probe pulse has been applied here, this will be addressed in Figure 3.)

prototypical D_2^+ may be optimally obtained for control pulse intensities $> 5 \times 10^{13} \text{ W cm}^{-2}$. In order to achieve an experimental realisation of control, a technique for characterising the modified wavepacket must be chosen. In recent examples, Coulomb explosion imaging has been outlined as a useful probe of a vibrationally quenched distribution^[15,22].

Complementary to this, theoretical results will be used here to demonstrate that fragmentation through photodissociation (PD) can also provide a useful channel for experimentally tracking and characterising the coherent wavepacket distribution^[17]. Fourier analysis of the PD yield will be shown to provide extra information on the frequency components in the wavepacket. Finally, the wavepacket redistribution will be studied as a function of control pulse intensity and delay time, providing key constraints and parameters to be borne in mind for future experimental studies.

Creation and control of the D_2^+ vibrational wavepacket

The scheme for ultrafast creation, control and characterisation of a vibrational wavepacket in D_2^+ is displayed schematically in Figure 1.

First, a coherent vibrational wavepacket can be launched on the ground electronic ($1s\sigma_g$) surface of D_2^+ , in a superposition of vibrational states.

Experimentally this can be achieved by strong field ionisation of a gas target ($D_2 \rightarrow D_2^+$) through a few-cycle pulse interaction^[5,6], providing the pulse duration is shorter than the vibrational period of the ion^[10]. For the particular simulations reported here, we use a Franck-Condon projection (consistent with experiments in^[5,10] where the pump polarization was perpendicular to the molecular axis), although we note that other techniques for modelling the ionisation process (leading to non-FC distributions) are important for particular pulse parameters. For more details on the pumping process the reader is referred to discussions in^[16,17] and references therein. Regardless of

the exact vibrational distribution, this wavepacket will exist in a broad superposition of vibrational states and begins to evolve across the $1s\sigma_g$ potential.

Secondly, a control pulse can be applied to this wavepacket after a time τ_c , serving to steer the molecular motion and redistribute the vibrational state populations. This occurs due to a field-induced coupling between the ground electronic state ($1s\sigma_g$) and first excited state ($2p\sigma_u$) of D_2^+ . In the frequency domain, this control operation can be understood as a Raman process^[13] where small portions of wavepacket are transferred back and forth between $1s\sigma_g$ and $2p\sigma_u$ states. The outcome of this process is extremely dependent on the vibrational eigenstate phases^[16] at the point of wavepacket transfer and, depending on the timing of a control pulse wavepacket portions may be heated or cooled in this way. After the control pulse has elapsed, the modified wavepacket will possess a new distribution of vibrational states, leading to a unique subsequent evolution, as shown in^[14,17].

The wavepacket can then be probed after a variable time delay τ_p , leading to photodissociation (PD) of the molecule where the D_2^+ ion will fragment to give D and D^+ products. As will now be seen, this PD channel can provide an excellent technique for characterising the wavepacket.

Simulations of experimentally accessible wavepacket control

Using this pump-control-probe scheme, simulations have been carried out to establish the key observables and constraints for future experimental studies. The numerical modelling was carried out within the Born-Oppenheimer and dipole approximations, with full details of the model given elsewhere^[14,16,17]. In brief, the D_2^+ vibrational wavepacket is propagated on the $1s\sigma_g$ potential through a Taylor expansion of the time-evolution operator, executed on a finite difference grid in R. The application of the laser pulse is included through a time dependent coupling term in the system Hamiltonian, expressed through two coupled equations given in^[17]. The wavepacket is then propagated beyond the application of the control pulse and the final vibrational amplitudes are extracted via overlap integral of the modified wavepacket with the basis set of D_2^+ eigenstates.

Prior to a control pulse, our wavepacket is in a Franck-Condon distribution of states in D_2^+ , as shown in Figure 2(a). The effect of the control pulse on the vibrational distribution was modelled for a pulse of $1 \times 10^{14} \text{ W cm}^{-2}$ peak intensity and 12 fs duration. The time evolving laser field contributes a dipole interaction term to the system Hamiltonian and the electric field profile is taken to span a Gaussian envelope (12 fs fwhm) with a carrier field of 800 nm light. The resulting distributions are shown in Figure 2 for a control pulse centred on (b) 20 fs, (c) 25 fs and (d) 30 fs respectively. It can be seen that the final distribution is strongly dependent on τ_c , with (b) cooling or (d) heating of the wavepacket occurring. This outcome has been well established in the recent literature^[13-16].

With these three (arbitrarily chosen) examples of control-driven vibrational redistribution at hand, an experimentally accessible technique for detailed

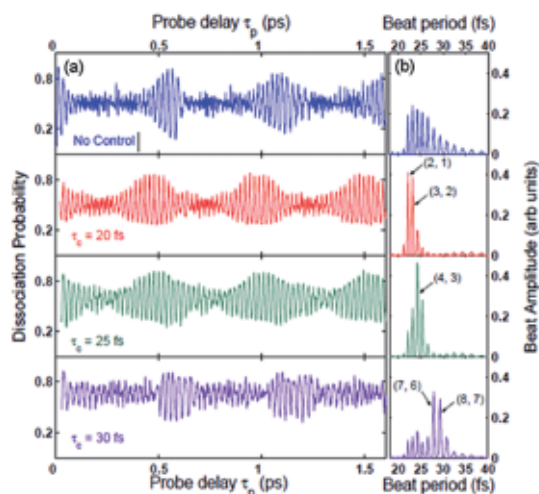


Figure 3. (a) Dissociation probability as a function of probe pulse delay time, τ_p for the distributions in Figure 2. Again, a 12 fs control pulse of 1×10^{14} W cm $^{-2}$ peak intensity has been applied for delay times of 20 fs, 25 fs and 30 fs. The yield peaks when the wavepacket is near the outer turning point in R and dips when the wavepacket is at small R. (b) FFT analysis extracts the vibrational beat components contributing to the wavepacket motion, providing experimentally accessible means for characterising the vibrational distribution.

characterisation must be considered. As a useful observable for the experimentalist to utilise, we model the probability of molecular dissociation arising from a probe pulse interaction at time τ_p . As the PD process exhibits an R dependence (enhanced near the outer turning point of the $1s\sigma_g$ well), the PD yield will be modulated as a function of τ_p , due to the evolution of the coherent wavepacket.

This has been modelled for each of the cases shown in Figure 2, where the corresponding wavepackets were propagated and the dissociation was predicted as a function of delay time τ_p . For this, the PD process was modelled for a 12 fs pulse (peak intensity 3×10^{14} W cm $^{-2}$) using the convenient 'critical R cut-off' (CRC) approximation introduced in^[17], which obviates the need for intensive quantum simulations of molecular dissociation. The corresponding PD yields are displayed in Figure 3(a). It is clear that the different vibrational distributions infer different trends in the respective PD yields, with the de-phasing and optimal re-phasing ('revival') conditions being enhanced at different τ_p values. The change in the revival structures provides an easily observable parameter for experimental studies and should infer whether or not the wavepacket has been modified in a state-selective manner via the control pulse. However, it does not provide a clear indication of which vibrational states are occupied.

Such characterisation can be achieved via Fourier analysis of the PD yield. To demonstrate the plausibility of this technique for future experimental studies, we have applied an FFT algorithm to the data in Figure 3(a), obtaining a spectral profile containing the dominant frequencies present in the PD signal. Since the PD signal provides a measure of the oscillation of the wavepacket, the FFT analysis provides the frequencies of the different wavepacket

components that oscillate back and forth in R. These are the beat frequencies $\omega_{v,v'}$ ^[17] and have been represented in Figure 3 (b). For convenience, the beat periods ($T_{v,v'} = 2\pi/\omega_{v,v'}$) have been plotted here to provide an accessible measure of the timescale on which the molecule evolves.

For example $\omega_{2,1}$ corresponds to the beat between $v=2$ and $v=1$ and provides a wavepacket component that oscillates in R with a period of 22 fs. The relative peak heights of the beat components are proportional to the populations in the occupied states and thus provide a measure of the vibrational distribution.

It can be clearly seen that there is excellent correlation between the beats observed in Figure 3(b) and the corresponding distributions in Figure 2. For example, if $\tau_c = 20$ fs the resulting wavepacket is enhanced in $v = 1, 2, 3$ and the corresponding PD-FFT technique reflects this, displaying the beats $\omega_{2,1}$ and $\omega_{3,2}$. It is worth noting that in such a wavepacket there is a beat term $\omega_{3,1}$ but this higher order beat occurs on a shorter timescale than shown here, and will be more difficult to resolve in experiments.

Effect of control pulse intensity and delay time

As seen in Figure 2, the vibrational distribution is sensitive to τ_c . This dependence has been studied in more detail for the 12 fs, 1×10^{14} W cm $^{-2}$ control pulse across a range of τ_c values from 10 - 55 fs in steps of 1/4 fs. At each τ_c value a full wavepacket propagation was carried out and the final vibrational distribution extracted, providing the results in Figure 4 (b).

This was also conducted for intensities of (a) 5×10^{13} (c) 2×10^{14} (d) 3×10^{14} and (e) 4×10^{14} W cm $^{-2}$, to provide a measure of the final vibrational distribution as a function of both peak intensity and τ_c . We choose to

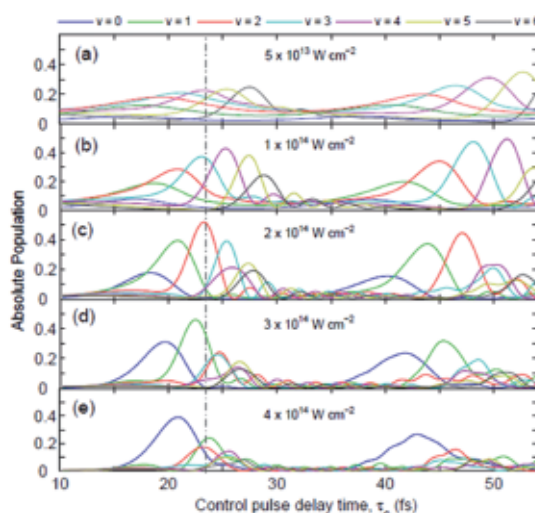


Figure 4. Final vibrational population for $v = 0-6$ as a function of τ_c for a pulse of 12 fs duration. At each τ_c value the wavepacket was propagated and the control pulse interaction was modelled with the resulting vibrational distribution extracted. Calculations were separately carried out for each of the control pulse intensities shown. As an example, the control pulse delay of $\tau_c = 23.5$ fs is marked (vertical dashed line) in order to highlight that the final distribution is extremely sensitive to the control pulse intensity.

focus on $v = 0-6$, as the most significant redistribution effects occur in these levels.

It is interesting to observe that carefully chosen intensities and τ_c parameters can lead to selectively tailored distributions. For example, a $3 \times 10^{14} \text{ W cm}^{-2}$ at $\tau_c = 24 \text{ fs}$ will give $v=1,2,3$ or alternatively a superposition of $v=3,4$ can be created at $\tau_c = 49.5 \text{ fs}$ for a $1 \times 10^{14} \text{ W cm}^{-2}$ pulse. Single state enhancements may also be achieved, e.g. $v=2$ at $\tau_c = 47 \text{ fs}$ in (c).

Consider the control delay of $\tau_c = 23.5 \text{ fs}$. In (b) a superposition of $v=3,4$ is obtained whereas (c) is predominantly in $v=2$ and (d) is $v=1$! Therefore at a given τ_c value the sensitivity of the control mechanism to the intensity of the pulse is clearly important. This raises two concerns for experimental applications. Firstly, the intensity at-focus must be well known.

This can actually be quite difficult to characterise for the on-target focussed pulse, however one possibility is to use an in-situ pump-probe technique to study multiple ionisation yields from a xenon target^[23], availing of interference effects to characterise at-focus pulse intensity and duration. Secondly, the effect of focal volume averaging may play a role and this must be carefully considered for the geometries and techniques involved in each experimental arrangement. So it is paramount that this intensity dependence for a chosen τ_c must be borne in mind for any future experiments.

Conclusions

Ultrafast control of a D_2^+ vibrational wavepacket has been simulated in order to identify key parameters and observables to direct future experimental efforts. Within a pump-control-probe scheme, the PD yield has been simulated for wavepackets that have been controlled at different τ_c values, with noticeable differences evident in the re-phasing and de-phasing structures. For different τ_c it has been shown that the position of the revival could change dramatically and the new superposition may also be characterised by the FFT of the PD yield.

This study has provided clear experimental observables to be sought in the PD channel for future pump-control-probe experiments on D_2^+ vibrations.

With this in mind, the effects of the pulse intensity and control delay on the D_2^+ vibrational distribution were investigated. For the delay times considered here (10-55 fs), the simulations imply that the control process can be sensitive to the intensity. This has been highlighted so that any future experimental efforts should place an importance on characterising the peak intensity and any focal volume effects that may occur systematically in the experimental technique.

Acknowledgements

RB King and L Graham acknowledge funding from the Department for Employment and Learning (NI). JD Alexander acknowledges funding from the European Social Fund. O Kelly and CR Calvert acknowledge funding from the Leverhulme trust and GRAJ Nemeth acknowledges funding from the STFC.

References

1. H. Stapelfeldt and T. Seideman, *Rev. Mod. Phys.* **75**, 543 (2003).
2. M. F. Kling *et al.*, *Science* **312**, 246 (2006).
3. D. S. Murphy *et al.*, *J. Phys. B* **40**, 2607 (2007).
4. T. Brixner and G. Gerber, *Chem. Phys. Chem.* **4**, 418 (2003).
5. J. McKenna *et al.*, CLF Annual Report p84 (2005/2006).
6. J. Wood *et al.*, CLF Annual Report p88 (2005/06).
7. A. Rudenko *et al.*, *Chem. Phys.* **329**, 193 (2006).
8. J. McKenna *et al.*, *J. Mod. Opt.* **54**, 1127.
9. Th. Ergler *et al.*, *Phys. Rev. Lett.* **97**, 193001 (2006).
10. W. A. Bryan *et al.*, *Phys. Rev. A*, **76**, 053402 (2007).
11. I. A. Bocharova *et al.*, *Phys. Rev. A*, **77**, 53407 (2008).
12. F. Légare *et al.*, *Phys. Rev. A*, **72**, 052717 (2005).
13. H. Niikura *et al.*, *Phys. Rev. Lett.*, **92**, 133002 (2004).
14. D. S. Murphy *et al.*, *New J of Phys.*, **9**, 260 (2007).
15. T. Niederhausen and U. Thumm, *Phys. Rev. A*, **77**, 013407 (2008).
16. C. R. Calvert *et al.*, *J. Phys. B*, **41**, 205504 (2008).
17. C. R. Calvert *et al.*, *J. Mod. Opt.* **56**, 91060 (2009).
18. W. A. Bryan *et al.*, 2009, submitted.
19. R. B. King *et al.*, CLF Annual Report (2007/2008).
20. C. R. Calvert *et al.*, CLF Annual Report p57 (2006/07).
21. H. Niikura *et al.*, *Phys. Rev. A*, **73**, 021402 (2006).
22. U. Thumm *et al.*, *Phys. Rev. A*, **77** 063401 (2008).
23. W. A. Bryan, CLF Annual Report p71 (2005/2006).